Applied Catalysis B: Environmental 218 (2017) 1–8

Contents lists available at ScienceDirect

Applied Catalysis B: Environmental

journal homepage: www.elsevier.com/locate/apcatb

Original research paper

Hydrogen production by ammonia decomposition over Cs-modified Co_3Mo_3N catalysts

Atthapon Srifa, Kaname Okura, Takeou Okanishi, Hiroki Muroyama, Toshiaki Matsui, Koichi Eguchi*

Department of Energy and Hydrocarbon Chemistry, Graduate School of Engineering, Kyoto University, Nishikyo-ku, Kyoto 615-8510, Japan

ARTICLE INFO

Article history:
Received 24 January 2017
Received in revised form 9 June 2017
Accepted 12 June 2017
Available online 13 June 2017

Keywords:
Ammonia decomposition
Co_3Mo_3N
Cesium
Hydrogen production

ABSTRACT

The Cs-modified Co_3Mo_3N catalysts were successfully prepared by a facile single-step decomposition of a mixture containing hexamethylenetetramine (HMTA) and corresponding metal salts under the flow of nitrogen at 700 °C and their catalytic activity for ammonia decomposition was investigated. The Co_3Mo_3N phase was observed in the XRD pattern of as-prepared sample and acted as the active component for the reaction. The XPS analysis clarified the existence of Cs species, indicating that these species should be dispersed over Co_3Mo_3N. The addition of a small amount of Cs species significantly improved the catalytic performance of the Co_3Mo_3N catalyst. The further addition of Cs species had a negative effect on the catalytic activity for the reaction. $^{15}NH_3$ isotopic studies revealed that the nitrogen species in Co_3Mo_3N were exchangeable with nitrogen atoms in gas phase, elucidating the mechanism of the reaction over the Co_3Mo_3N catalysts. The kinetics analysis indicated that the modification by a small amount of Cs species alleviated the negative effect of the hydrogen poisoning on the active sites of Co_3Mo_3N catalysts. The desorption behavior of hydrogen and nitrogen suggested that the Cs modification facilitated the recombinative desorption of hydrogen and nitrogen atoms from the active components, resulting in the improvement in the activity of Co_3Mo_3N. This improvement was due to the electronic modification of Co_3Mo_3N by the electron donation of Cs promoter.

1. Introduction

In recent years, ammonia has been considered as one of the hydrogen sources because of many advantages such as high volumetric energy density, low production cost, and CO_x-free hydrogen production. In particular, it can be liquefied under mild conditions (−33.4 °C at atmospheric pressure or 8.46 atm at 20 °C) [1–4]. Ammonia decomposes into hydrogen and nitrogen at 400 °C according to the thermodynamic calculation (equilibrium conversion ≈ 99%), at which hydrocarbon steam reforming reactions provide the low hydrocarbon conversion and hydrogen production yield [5].

Various metal catalysts such as Ru, Ir, Rh, Pd, Pt, Ni, Co, and Fe supported on Al_2O_3, carbon nanotube (CNT), activated carbon (AC), SiO_2, MgO, ZrO_2, TiO_2, and rare earth oxides have been intensively investigated for ammonia decomposition reaction [6–14]. Among these catalysts, Ru catalysts supported on multi-wall carbon nanotube are the most active for ammonia decomposition [8]. Besides, Ru nanoparticles embedded into a lanthanum-stabilized zirconia (LSZ) support were found to be active and stable catalysts for the reaction due to the minimization of undesirable sintering of the Ru nanoparticles [15]. In addition, Ru incorporated SiO_2 type nanocomposite catalyst with a particle size of 4–10 nm was highly effective at high flow rate of ammonia [14].

Alkali and alkaline earth metals such as Na, K, Rb, Cs, Ca, Sr, and Ba have been studied as a promoter for the reaction [5,10,16–18]. The Ru catalyst supported on graphitized carbon nanotubes with an electron donating promoter of Cs has high ammonia decomposition activity at low reaction temperature (below 400 °C) [16]. This is because the electronic modification of the active sites by Cs species can facilitate the nitrogen recombinative desorption on the Ru surface [10]. However, the hydrogen poisoning effect on the active sites inhibited the ammonia decomposition over Ru-based catalysts [6,19–21]. In addition, the high cost and limited availability of Ru obstruct the large-scale applications. Therefore, it is necessary to develop inexpensive and highly active catalysts based on non-noble metals.

* Corresponding author.
E-mail address: eguchi@scl.kyoto-u.ac.jp (K. Eguchi).

http://dx.doi.org/10.1016/j.apcatb.2017.06.034
0926-3373/

Less expensive transition metal nitrides with the similar characteristic to noble metals have attracted attention as the effective catalysts in different reactions such as hydrogenation [22], hydrodenitrogenation [23], hydrodesulfurization [24,25], Fischer-Tropsch synthesis [26], and ammonia synthesis [27] and decomposition [7,28–32]. It is well-know that the metal-nitrogen interaction plays as a crucial role in ammonia synthesis and decomposition because the adsorption and desorption of nitrogen involve in the rate determining steps of synthesis and decomposition of ammonia, respectively [33]. Transition metal nitrides such as VN, Mo_2N, and Fe_3N have been investigated for the ammonia decomposition reaction [30,34]. Among them, much attention has been devoted to the Mo nitride-based catalysts for the ammonia decomposition reaction due to the low cost and high activity. Furthermore, ternary nitrides such as Co_3Mo_3N, Ni_2Mo_3N, Ni_3Mo_3N, and Fe_3Mo_3N catalysts have been suggested as the highly active species for the ammonia decomposition reaction [28,30,35–37]. We have recently demonstrated that the Co_3Mo_3N catalyst exhibits the highest activity for ammonia decomposition among various Mo nitride-based ones [32].

As mentioned above, the addition of base metal species to catalysts enhances their activity for ammonia decomposition. However, to the best of our knowledge, the additive effect of basic species on the catalytic activity of metal nitrides has not been fully investigated so far. In this present work, the Cs-modified Co_3Mo_3N catalysts were successfully prepared by a single-step decomposition of mixture containing hexamethylenetetramine (HMTA) and corresponding metal salts, and their catalytic activity for ammonia decomposition was investigated. The catalysts were characterized by N_2 adsorption, X-ray diffraction (XRD), X-ray photoelectron spectroscopy (XPS), and transmission electron microscopy (TEM). The isotopic studies by $^{15}NH_3$ pulse reaction were conducted in order to further comprehend the reaction mechanism of ammonia decomposition over the nitride-based catalysts. Besides, the kinetics analysis was carried out in order to examine the influence of ammonia, hydrogen, and nitrogen on catalytic reaction. Moreover, the desorption processes of reactant and products were elucidated by NH_3-temperature programmed surface reaction (NH_3-TPSR) measurements.

2. Experimental section

2.1. Catalyst preparation

Cobalt (II) nitrate hexahydrate [$Co(NO_3)_2{\cdot}6H_2O$, purity 98.0%], ammonium heptamolybdate [$(NH_4)_4Mo_7O_{24}{\cdot}4H_2O$, purity 99.0%], cesium nitrate [$CsNO_3$, purity 99.9%], hexamethylenetetramine [$C_6H_{12}N_4$, purity 99.0%], and 25% ammonia solution were obtained from Wako Pure Chemical Industries, Ltd., Japan. All chemicals were used without further purification.

In this work catalyst preparation was adapted according to the route described previously [38]. A mixture for the Cs-modified Co_3Mo_3N catalysts were prepared by dissolving $Co(NO_3)_2{\cdot}6H_2O$, $(NH_4)_4Mo_7O_{24}{\cdot}4H_2O$, and HMTA with a fixed molar ratio of 14:2:34 in 15% NH_3 solution. The solution was stirred for 3 h and then the $CsNO_3$ with different amount was added into the solution. Subsequently, the solution was evaporated slowly to dryness. Finally, the sample was dried in air at 60 °C overnight and then calcined in a tube furnace under a flow of N_2 at a rate of 50 $cm^3\ min^{-1}$ at 700 °C for 5 h. The Cs-modified Co_3Mo_3N with a molar ratio of $Cs{:}Co_3Mo_3N = x{:}1$ is labeled as $Cs_xCo_3Mo_3N$ (x = 0, 0.006, 0.009, 0.018, 0.027, 0.036, 0.18, and 0.24).

2.2. Catalyst characterizations

Powder X-ray diffraction (XRD) patterns of the samples were collected on an X-ray diffractometer (XRD, Rigaku, Ultima IV X-ray diffractometer) using Cu Kα radiation. The measurement was operated at 40 kV and 40 mA with a scanning rate of 20° min^{-1} in the 2θ range of 10–80°.

X-ray photoelectron spectroscopy (XPS) analysis was performed on a JEOL, JPS-9200 equipped with Mg Kα radiation source. The binding energies were calibrated with respect to signal for C 1s at 285 eV.

The BET surface area and total pore volume of the samples were measured at −196 °C with a nitrogen adsorption-desorption technique (BEL Japan, Bellsorp-miniII). Prior to measurement, the samples were pretreated at 150 °C for 3 h. The specific surface area was determined based on the BET approach. The total pore volume was measured at the relative pressure (P/P_0) of 0.98.

The ammonia temperature-programmed surface reaction (NH_3-TPSR) was performed to elucidate the desorption behavior of the reactant and product species during the ammonia decomposition. Prior to the NH_3-TPSR measurements, the catalysts were pretreated at 500 °C in pure H_2 flow (30 $cm^3\ min^{-1}$) for 1 h, followed by in pure NH_3 flow (30 $cm^3\ min^{-1}$) for 1 h at atmospheric pressure. After cooling to 50 °C, NH_3 adsorption was conducted in pure NH_3 for 1 h, followed by the gas replacement by He for 1 h. The NH_3-TPSR was conducted by raising the temperature from 50 to 1000 °C at a heating rate of 10 °C min^{-1} with a supply of He at a rate of 30 $cm^3\ min^{-1}$. The desorbed NH_3, H_2, and N_2 were monitored by an online mass spectrometer (Pfeiffer Vacuum, OmniStar GSD320).

The morphology and particle size of the catalysts were examined by a transmission electron microscope (TEM, JEOL, JEM-2100F) equipped with an energy dispersive X-ray spectrometer (EDS, JED-2300T, JEOL). The average Co_3Mo_3N particle size was evaluated from at least 100 particles.

2.3. Ammonia decomposition activity measurements

The ammonia decomposition activity and stability were evaluated in a fixed-bed reactor. The catalyst powder was uniaxially-pressed at 30 MPa and were pulverized to 0.3-0.85 mm diameter. The catalysts (0.3 g) were loaded into the reactor and then were pretreated at 500 °C in the flow of H_2 for 1 h, followed by pure NH_3 for 1 h. The reaction activity test was carried out with a supply of pure ammonia at a space velocity of 6000 l $kg^{-1}\ h^{-1}$ in the heating process. The catalytic activity for ammonia decomposition was investigated in the range of 300–600 °C; meanwhile the stability of the catalyst was studied at 500 °C. The outlet gas was passed through two traps containing H_2SO_4 solution (Wako Pure Chemical Industries) to remove the unreacted NH_3. Then the flow rate of outlet gas was measured by using a flow meter (VP3, Horiba STEC Co, Ltd.). Therefore, the ammonia conversion was calculated as the following equation according to the assumption that the resulting gas was composed of N_2 and H_2.

$$NH_3\ conversion\ (\%) = \frac{F_{out}}{2F_{in}} \times 100 \quad (1)$$

Where F_{in} and F_{out} are the flow rates of inlet and outlet gases, respectively.

In addition, the kinetics analysis was conducted for Mo nitride-based catalysts at 450 °C and a space velocity of 10,000 l $kg^{-1}\ h^{-1}$ by varying the partial pressure of ammonia, hydrogen, or nitrogen (NH_3: 10–30 vol.%, H_2: 10–30 vol.%, N_2: 10–30 vol.%, and Ar balance).

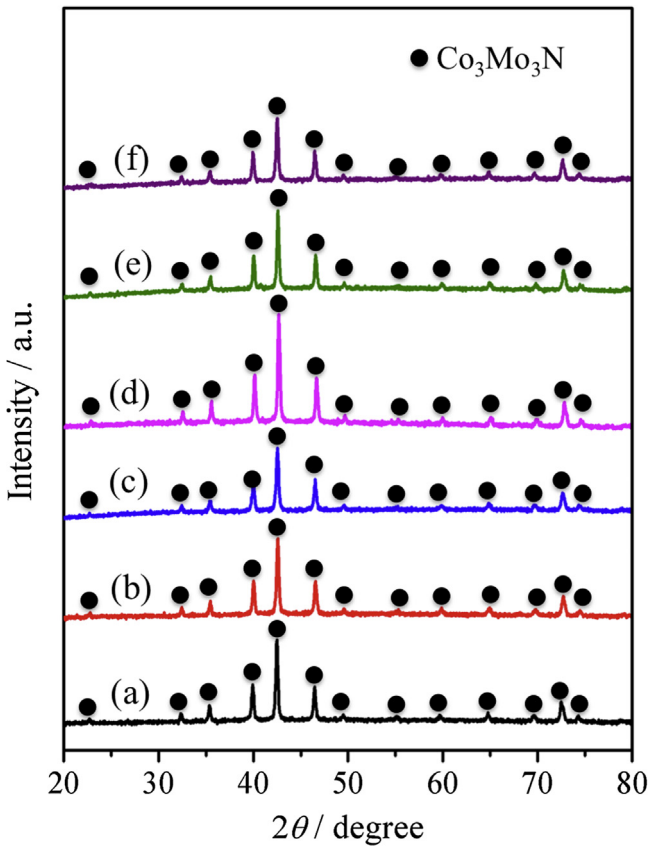

Fig. 1. X-ray diffraction patterns of the fresh (a) Co_3Mo_3N, (b) $Cs_{0.006}Co_3Mo_3N$, (c) $Cs_{0.009}Co_3Mo_3N$, (d) $Cs_{0.018}Co_3Mo_3N$, (e) $Cs_{0.027}Co_3Mo_3N$, and (f) $Cs_{0.036}Co_3Mo_3N$ catalysts.

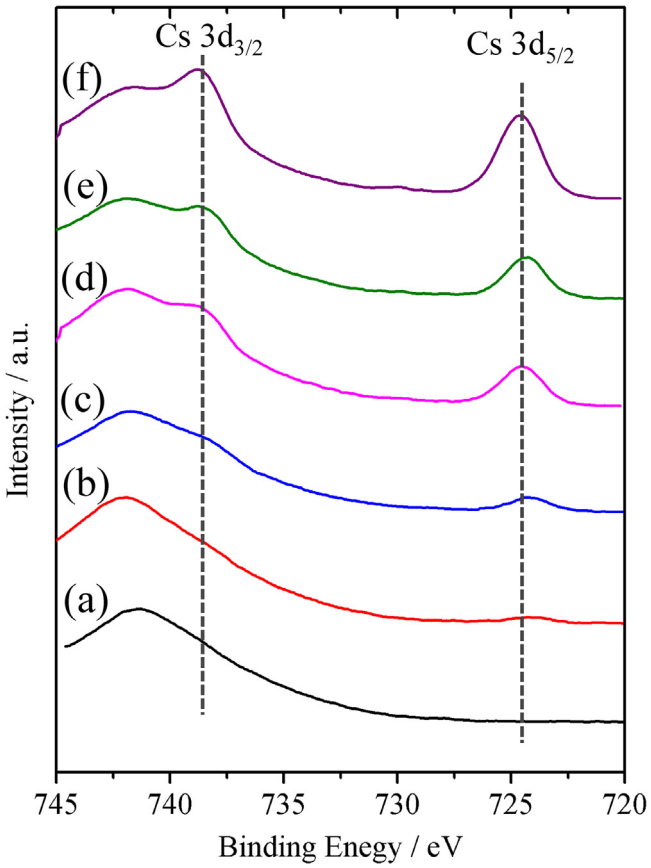

Fig. 2. Cs 3d spectra for the fresh (a) Co_3Mo_3N, (b) $Cs_{0.006}Co_3Mo_3N$, (c) $Cs_{0.009}Co_3Mo_3N$, (d) $Cs_{0.018}Co_3Mo_3N$, (e) $Cs_{0.027}Co_3Mo_3N$, and (f) $Cs_{0.036}Co_3Mo_3N$ catalysts.

2.4. Isotopic studies by $^{15}NH_3$ pulse method

Isotopic studies were carried out with $^{15}NH_3$ pulse method for unmodified and modified samples to elucidate the reaction mechanism over the nitride-based catalysts. Prior to the reaction, the synthesized catalysts were pre-treated at 500 °C in pure H_2 flow (30 cm^3 min^{-1}) for 1 h, followed by pure $^{14}NH_3$ flow (30 cm^3 min^{-1}) for 1 h. The pulse of $^{15}NH_3$ (98% ^{15}N) (50 μL) was injected into He flow (30 cm^3 min^{-1}) at 500 °C for 10 times to expose the sample. Subsequently, after cooling to 50 °C in He, the sample was heated from 50 to 1000 °C at a rate of 10 °C min^{-1} with a supply of He at a rate of 30 cm^3 min^{-1}. The desorption of gas species was detected by an online mass spectrometer (Pfeiffer Vacuum, OmniStar GSD320).

3. Results and discussion

3.1. Structural and textural properties of the Cs-modified Co_3Mo_3N catalysts

We have previously shown that the non-precious Co_3Mo_3N exhibits higher activity for ammonia decomposition than Mo_2N, Ni_3Mo_3N, and Fe_3Mo_3N catalysts [32]. In this study, a series of Cs-modified Co_3Mo_3N catalysts was successfully prepared by a single-step decomposition of mixture containing HMTA and corresponding metal salts under the flow of nitrogen at 700 °C. The molar ratio of Cs to Co_3Mo_3N was varied in the range of 0–0.24. The characteristics of the catalysts were investigated. The phase identification and crystallinity of the synthesized samples were analyzed through XRD. Fig. 1 shows the XRD patterns of the unmodified and the Cs-modified Co_3Mo_3N catalysts. The diffraction pattern of all the catalysts consisted of the pure phase of Co_3Mo_3N (PDF#01-072-6570). The impurity phases were not detectable by XRD. Besides, no characteristic diffraction peaks of Cs species were observed, implying that the small particles of Cs species should be highly dispersed on the Co_3Mo_3N surface. Then, the XPS measurement was used to examine the presence of Cs species onto the catalyst surface. The XPS spectra of Cs 3d for the unmodified and modified samples are depicted in Fig. 2. The characteristic peaks of Cs 3d appeared at Cs $3d_{3/2}$ = 738.7 eV and Cs $3d_{5/2}$ = 724.4 eV for all the modified catalysts, indicating that the Cs species predominately existed in the form of Cs_2O [39,40]. This finding would confirm that the Cs species existed on the surface of catalysts for all the Cs-modified Co_3Mo_3N samples.

In addition, the XRD and XPS measurements of the spent Co_3Mo_3N, $Cs_{0.009}$ Co_3Mo_3N, and $Cs_{0.018}Co_3Mo_3N$ catalysts were conducted as shown in Figs. S1 and S2, respectively. The XRD confirmed that the phase of Co_3Mo_3N was still present for all the samples after the stability test for 100 h. Similarly, the XPS spectra of Cs 3d for modified samples exhibited the existence of Cs species after the stability test for 100 h. These implied that the structure of Cs-modified Co_3Mo_3N catalysts was highly stable in ammonia decomposition.

The N_2 adsorption–desorption measurements were conducted to examine the textural properties of the catalysts. Table 1 lists the BET specific surface area and pore volume of the unmodified Co_3Mo_3N and the series of Cs-modified Co_3Mo_3N catalysts. The N_2 adsorption–desorption isotherm of all the catalysts exhibited a type I or II without hysteresis loop, indicating the characteristic of the large mesopores or macropores (not shown). This generally resulted from the voids between the primary particles constituting the main bulk phases [28,41]. The BET surface area of the

Table 1
BET surface area and pore volume of the Cs-modified Co_3Mo_3N catalysts.

Catalyst	BET surface area[a] ($m^2\,g^{-1}$)	Pore volume[b] ($cm^3\,g^{-1}$)
Co_3Mo_3N	9.1	0.0079
$Cs_{0.006}Co_3Mo_3N$	8.1	0.0070
$Cs_{0.009}Co_3Mo_3N$	8.2	0.0070
$Cs_{0.018}Co_3Mo_3N$	8.2	0.0070
$Cs_{0.027}Co_3Mo_3N$	8.3	0.0068
$Cs_{0.036}Co_3Mo_3N$	7.4	0.0060

[a] BET surface area calculated from the adsorption branch of the N_2 isotherm.
[b] Total pore volumes calculated from the N_2 adsorption at a relative pressure of 0.98.

unmodified Co_3Mo_3N was 9.1 $m^2\,g^{-1}$ with the pore volume of 0.0079 $cm^3\,g^{-1}$. The BET surface area of Co_3Mo_3N, synthesized by temperature-programmed reaction of the $CoMoO_4$ with NH_3, was reported to be 6.1 $m^2\,g^{-1}$ [42], which was lower than that in this study. The addition of Cs into the Co_3Mo_3N species seems to decrease the catalyst surface area. However this is possible with the experimental error, and there are not evidences to suggest that Cs species was incorporated in the pores of the Co_3Mo_3N species. Furthermore, as shown in Table S1, after the stability test at 500 °C for 100 h, the BET surface area and pore volume of the spent catalysts did not significantly change. This suggests that the textural properties of the catalysts were highly stable in the presence of ammonia.

To investigate the morphology and particle size of the prepared samples, typical TEM images of the Co_3Mo_3N, $Cs_{0.009}Co_3Mo_3N$, and $Cs_{0.018}Co_3Mo_3N$ catalysts are represented in Fig. 3. The particles of all the selected catalysts were in various sizes and could be partially distinguished between each other. These seem to merge with each other and the range of particle size distribution was 30–80 nm for all the samples. This suggested that the addition of a small amount of Cs species into the Co_3Mo_3N catalyst did not affect the morphology and size of Co_3Mo_3N particles. In addition, the elemental mapping analysis for the $Cs_{0.009}Co_3Mo_3N$ and $Cs_{0.018}Co_3Mo_3N$ samples based on TEM-EDS analysis revealed the clusters of Co and Mo species with the homogeneous distribution of Cs species (See in Fig. S3).

The CO_2-TPD measurement was conducted to evaluate the basic sites of the prepared catalysts. Fig. S4 shows the CO_2 ($m/z = 44$) desorption profiles in CO_2-TPD measurement over the Co_3Mo_3N and $Cs_{0.018}Co_3Mo_3N$ catalysts. A broad desorption peak of CO_2 was observed in the range of 170–425 °C for both samples. These peaks would be derived from the desorption of CO_2 on basic sites of the catalysts. The ion current of desorbed CO_2 for $Cs_{0.018}Co_3Mo_3N$ was higher than that for the unmodified Co_3Mo_3N. This suggested that the number of basic sites interacting with CO_2 increased by the addition of Cs into the Co_3Mo_3N catalyst (See in Table S2).

3.2. Catalytic performance for the Cs-modified Co_3Mo_3N catalysts

The catalytic performance of a series of Cs-modified Co_3Mo_3N catalysts for ammonia decomposition was examined at a gas space velocity of 60001 $kg^{-1}\,h^{-1}$. The contents of Cs in Co_3Mo_3N were varied with a molar ratio of Cs to Co_3Mo_3N in the range of 0–0.24. Fig. 4 shows the ammonia conversion in the temperature range of 300–600 °C for the catalysts. The ammonia conversion increased monotonically with the reaction temperature because of the endothermic nature of ammonia decomposition reaction as well as the enhancement of reaction rate based on the Arrhenius law. It can be seen that all the catalysts exhibited almost 100% of ammonia conversion at 550 °C. However, the difference in the catalytic performance was significant at lower temperatures of ca. 350–500 °C. Ammonia was converted over the

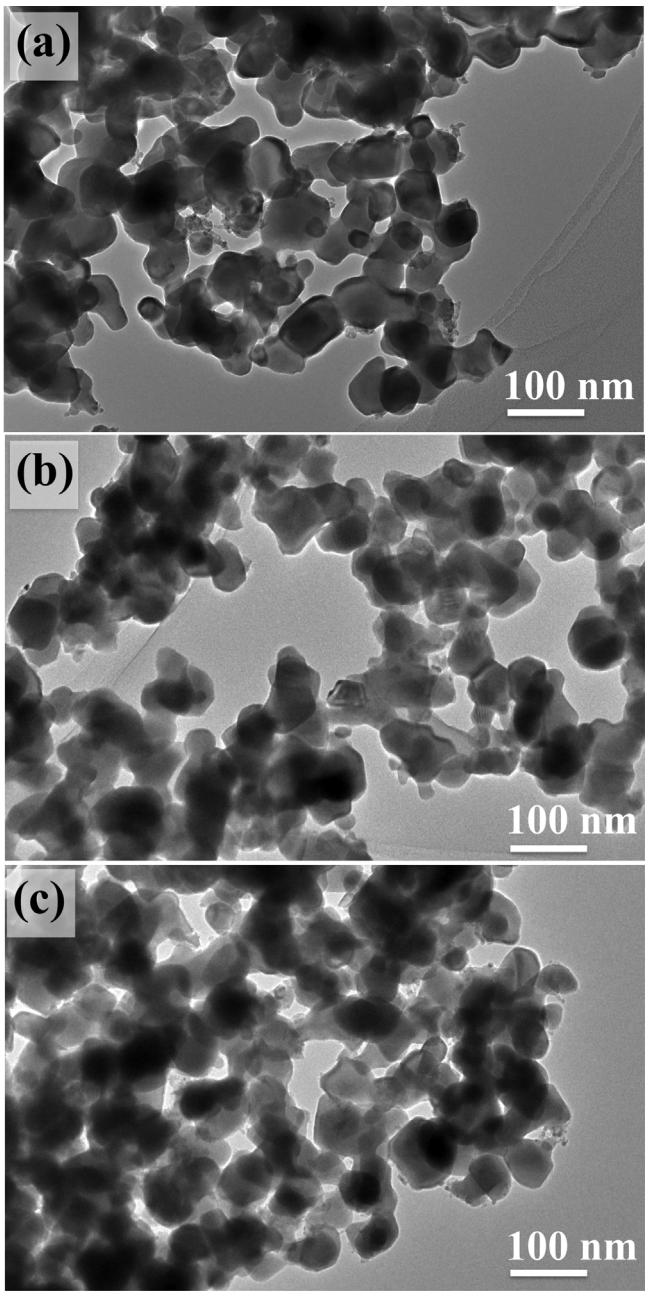

Fig. 3. TEM images of the fresh (a) Co_3Mo_3N, (b) $Cs_{0.009}Co_3Mo_3N$, and (c) $Cs_{0.018}Co_3Mo_3N$ catalysts.

Cs-modified Co_3Mo_3N catalysts from 350 °C. The ammonia conversion of unmodified catalyst was 61.2% at 500 °C, which was lower than that of the modified ones. For the Cs-modified Co_3Mo_3N catalysts, the ammonia conversion drastically increased with a rise in the molar ratio of Cs/Co_3Mo_3N from 0 to 0.018 in the temperature range of 350–500 °C. However the further increase in the Cs/Co_3Mo_3N ratio significantly decreased ammonia conversion. In particular, the samples with $Cs/Co_3Mo_3N = 0.18$ and 0.24 exhibited lower activity than the unmodified one (See in Fig. S5). The excess amount of Cs seemed to partially cover the active Co_3Mo_3N sites, leading to the reduction of hydrogen production rate. The highest conversion of the $Cs_{0.009}Co_3Mo_3N$ and $C_{0.018}Co_3Mo_3N$ catalysts attained ca. 94.7% at 500 °C. Hill et al. reported that the enhancement of Cs-Ru supported CNT was due to the electronic modification of Ru by the electron donating Cs promoter [10,16]. It should be noted the modification of Co_3Mo_3N by a small amount

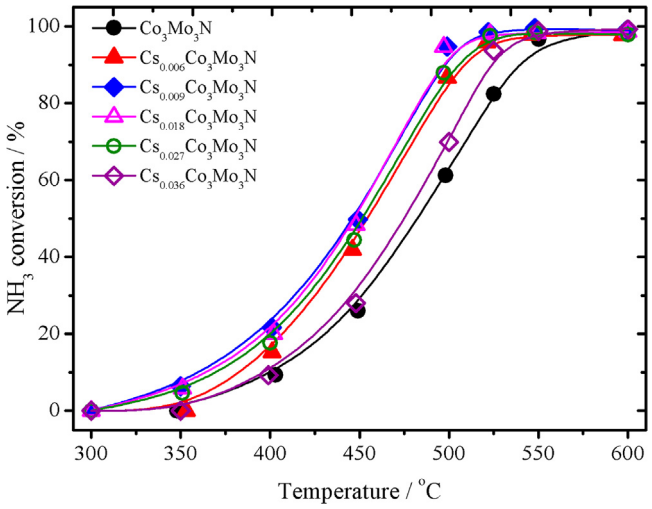

Fig. 4. Ammonia conversions at different temperature of the Co_3Mo_3N, $Cs_{0.006}Co_3Mo_3N$, $Cs_{0.009}Co_3Mo_3N$, $Cs_{0.018}Co_3Mo_3N$, $Cs_{0.027}Co_3Mo_3N$, and $Cs_{0.036}Co_3Mo_3N$ catalysts at a gas space velocity of 6000 l kg^{-1} h^{-1}.

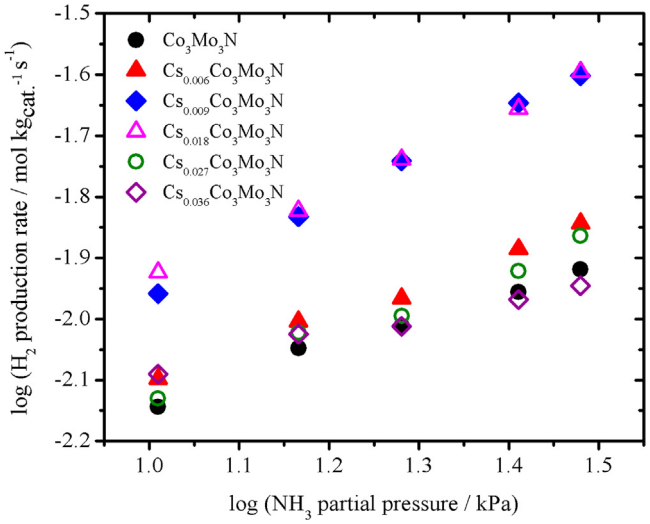

Fig. 5. Dependence of partial pressure of NH_3 on the reaction rate for ammonia decomposition over the Co_3Mo_3N, $Cs_{0.006}Co_3Mo_3N$, $Cs_{0.009}Co_3Mo_3N$, $Cs_{0.018}Co_3Mo_3N$, $Cs_{0.027}Co_3Mo_3N$, and $Cs_{0.036}Co_3Mo_3N$ catalysts at 450 °C. The partial pressure of NH_3 was varied from 10–30 vol.% with a constant space velocity of 10,000 l kg^{-1} h^{-1}.

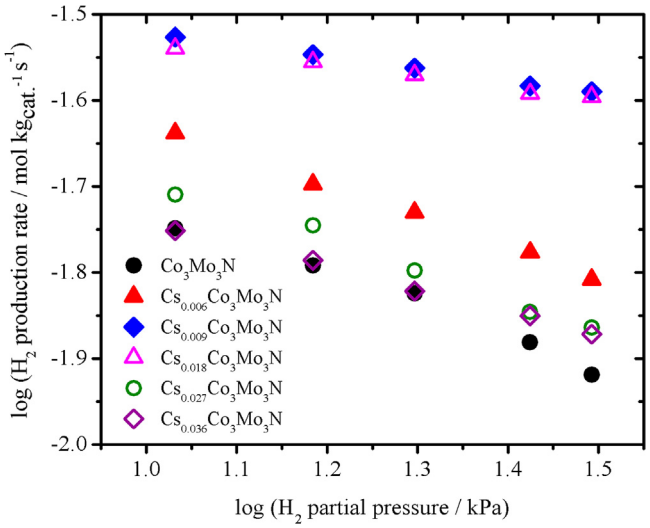

Fig. 6. Dependence of partial pressure of H_2 on the reaction rate for ammonia decomposition over the Co_3Mo_3N, $Cs_{0.006}Co_3Mo_3N$, $Cs_{0.009}Co_3Mo_3N$, $Cs_{0.018}Co_3Mo_3N$, $Cs_{0.027}Co_3Mo_3N$, and $Cs_{0.036}Co_3Mo_3N$ catalysts at 450 °C. The partial pressure of H_2 was varied from 10–30 vol.% with a constant space velocity of 10,000 l kg^{-1} h^{-1}.

of Cs species as electronic donating promoter was highly effective for ammonia decomposition reaction.

The kinetics analysis was conducted to examine the influence of the partial pressures of ammonia, hydrogen, and nitrogen on the reaction rate of ammonia decomposition reaction. The reaction orders for ammonia decomposition over the Cs-modified Co_3Mo_3N catalysts were evaluated at 450 °C. The partial pressures of ammonia, hydrogen, and nitrogen were varied in the range of 10–30 vol.% at a constant gas space velocity of 10,000 l kg^{-1} h^{-1}. The reaction orders of nitrogen over Co_3Mo_3N and $Cs_{0.018}Co_3Mo_3N$ catalysts were approximately zero (see in Fig. S6). This suggested that the nitrogen partial pressure did not affect the reaction rate. This result was consistent with the kinetics behavior of Ni, Ru, and Mo nitride-based catalysts reported previously [6,32,33,43]. Hence, the rate of ammonia decomposition was determined as the following equation.

$$r = kP_{NH_3}{}^{\alpha}P_{H_2}{}^{\gamma} \quad (2)$$

Where, k is a reaction rate constant, and α, and γ represent the reaction orders of ammonia and hydrogen, respectively.

Figs. 5 and 6 display the dependences of ammonia and hydrogen partial pressures on the reaction rate for ammonia decomposition over the unmodified and Cs-modified Co_3Mo_3N catalysts at 450 °C. The NH_3 conversion and reaction orders of ammonia and hydrogen for the Co_3Mo_3N modified by various amounts of Cs are summarized in Table 2. The reaction order with respect to ammonia (α) was positive for all the catalysts. The addition of a small amount of Cs species into Co_3Mo_3N enhanced this value. On the contrary, the reaction orders with respect to hydrogen (γ) were negative, implying that the generated hydrogen inhibited the ammonia decomposition over all the catalysts. The value of order γ was in the range from −1.0 to −0.5 for the Ni-based catalysts reported in the literatures [6,19]. The larger absolute value of order indicates a serious influence of hydrogen by its occupation on the active sites, resulting in the low catalytic activity. The absolute value decreased with a rise in the molar ratio of Cs/Co_3Mo_3N from 0.006 to 0.018. On the other hand, the further increase in Cs/Co_3Mo_3N ratio up to 0.036 provided almost the similar value as compared with the unmodified sample. Note that the Cs-modified Co_3Mo_3N catalysts with small amounts of additive exhibited less negative effect of the generated hydrogen. Therefore, it can be concluded that the modification of Co_3Mo_3N by a small amount of Cs species alleviated the hydrogen poisoning effect on ammonia decomposition.

A possible explanation for the reaction order is the weak adsorption of hydrogen on the surface of the catalyst by the electron donation from the Cs species. Meanwhile, a small amount of Cs species enhanced the reaction order of NH_3. This implies that ammonia should readily adsorb on the surface of Cs-modified Co_3Mo_3N.

3.3. Isotopic studies by $^{15}NH_3$ pulse method

In order to further comprehend the reaction mechanism over the nitride-based catalysts, the isotopic exchange reaction by $^{15}NH_3$ pulse method was performed for the $Co_3Mo_3{}^{14}N$ and $Cs_{0.018}Co_3Mo_3{}^{14}N$ catalysts. Fig. 7 shows the mass spectrometric signals for hydrogen and nitrogen species from ammonia decom-

Table 2
NH_3 conversion, reaction order, activation energy, and turnover frequency (TOF) over the Cs-modified Co_3Mo_3N catalysts.

Catalyst	NH_3 conversion (%)[a]	Reaction order[b]		Activation energy	TOF
		α	γ	(kJ mol^{-1})[c]	(mol NH_3 g_{cat}^{-1} s^{-1})[d]
Co_3Mo_3N	26.0	0.46	−0.36	86.2	0.70
$Cs_{0.006}Co_3Mo_3N$	41.9	0.53	−0.36	76.7	1.12
$Cs_{0.009}Co_3Mo_3N$	47.3	0.76	−0.14	65.1	1.27
$Cs_{0.018}Co_3Mo_3N$	48.3	0.69	−0.13	70.9	1.29
$Cs_{0.027}Co_3Mo_3N$	44.4	0.53	−0.35	71.4	1.19
$Cs_{0.036}Co_3Mo_3N$	28.1	0.29	−0.28	86.5	0.75

[a] Calculated at 450 °C and a space velocity of 60001 kg^{-1} h^{-1} (NH_3: 100 vol.%).
[b] Calculated at 450 °C and a space velocity of 10,0001 kg^{-1} h^{-1} (NH_3: 10–30 vol.%, H_2: 10–30 vol.%, and Ar balance).
[c] Calculated in the range of 400–500 °C and a space velocity of 60001 kg^{-1} h^{-1} (NH_3: 100 vol.%).
[d] Calculated at 450 °C and a space velocity of 60001 kg^{-1} h^{-1} (NH_3: 100 vol.%).

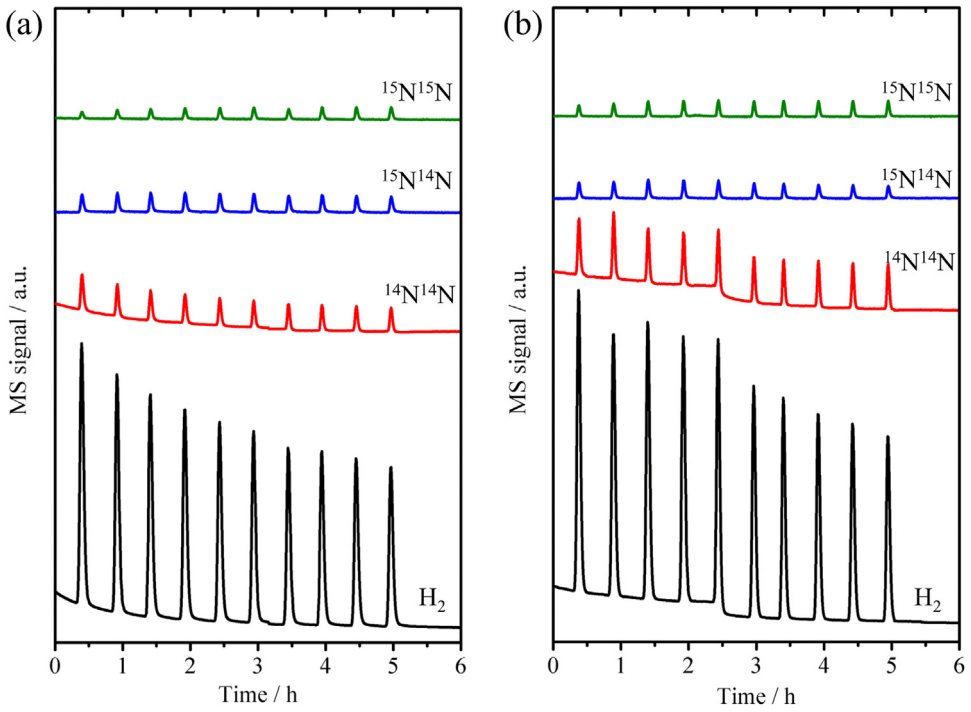

Fig. 7. H_2 (m/z = 2), $^{14}N^{14}N$ (m/z = 28), $^{15}N^{14}N$ (m/z = 29), and $^{15}N^{15}N$ (m/z = 30) profiles for the (a) $Co_3Mo_3{}^{14}N$ and (b) $Cs_{0.018}Co_3Mo_3{}^{14}N$ catalysts during the $^{15}NH_3$ pulse reaction at 500 °C.

position over both catalysts at 500 °C. After $^{15}NH_3$ injection, $^{15}NH_3$ was not detected for both catalysts, suggesting the complete ammonia decomposition. In contrast, the sharp peaks in the H_2, $^{14}N^{14}N$, $^{15}N^{14}N$, and $^{15}N^{15}N$ signals appeared with the similar behavior for unmodified and modified samples. This implies that the ^{14}N atoms in the catalysts were exchanged with the ^{15}N atoms in the injected $^{15}NH_3$. In ammonia decomposition, NH_3 molecules adsorb on the catalyst surface, followed by the dehydrogenation of NH_x species (x = 1–3). Nitrogen atoms generated from dehydrogenation combine and desorb as nitrogen molecules from the surface. In this test, a part of ^{14}N atoms in the catalysts were exchanged with the generated ^{15}N atoms in the vicinity of surface, and the ^{14}N and ^{15}N atoms produced $^{14}N^{14}N$ and $^{15}N^{14}N$ in addition to $^{15}N^{15}N$. After the pulse test, the Co_3Mo_3N sample was cooled down to 50 °C in He and subsequently heated from 50 to 1000 °C in He in order to confirm the N species in the sample. Fig. 8 displays the $^{14}N^{14}N$, $^{15}N^{14}N$, and $^{15}N^{15}N$ production profiles for the $Co_3Mo_3{}^{14}N$ catalyst. The $^{14}N^{14}N$, $^{15}N^{14}N$, and $^{15}N^{15}N$ molecules were detected above 650 °C. This result confirmed that the ^{15}N atom exchanged with ^{14}N atom in the catalyst. Therefore, it can be concluded that the nitrogen species in Co_3Mo_3N were exchangeable, elucidating the Mars-Van Krevelen reaction mechanism over the Co_3Mo_3N cat-

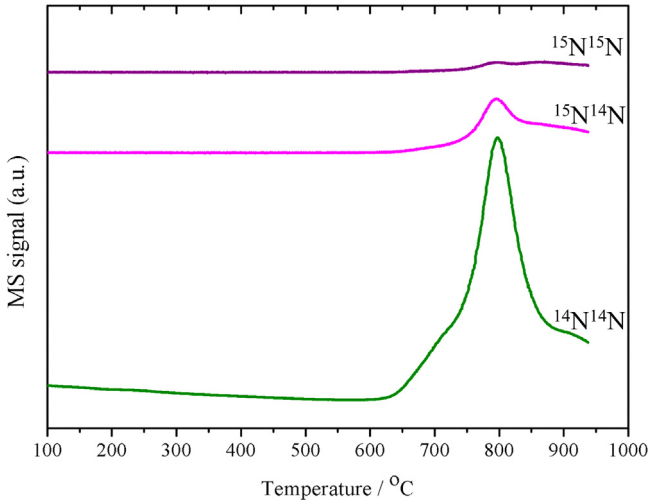

Fig. 8. $^{14}N^{14}N$ (m/z = 28), $^{15}N^{14}N$ (m/z = 29), and $^{15}N^{15}N$ (m/z = 30) profiles in He after $^{15}NH_3$ pulse reaction for the $Co_3Mo_3{}^{14}N$ catalyst.

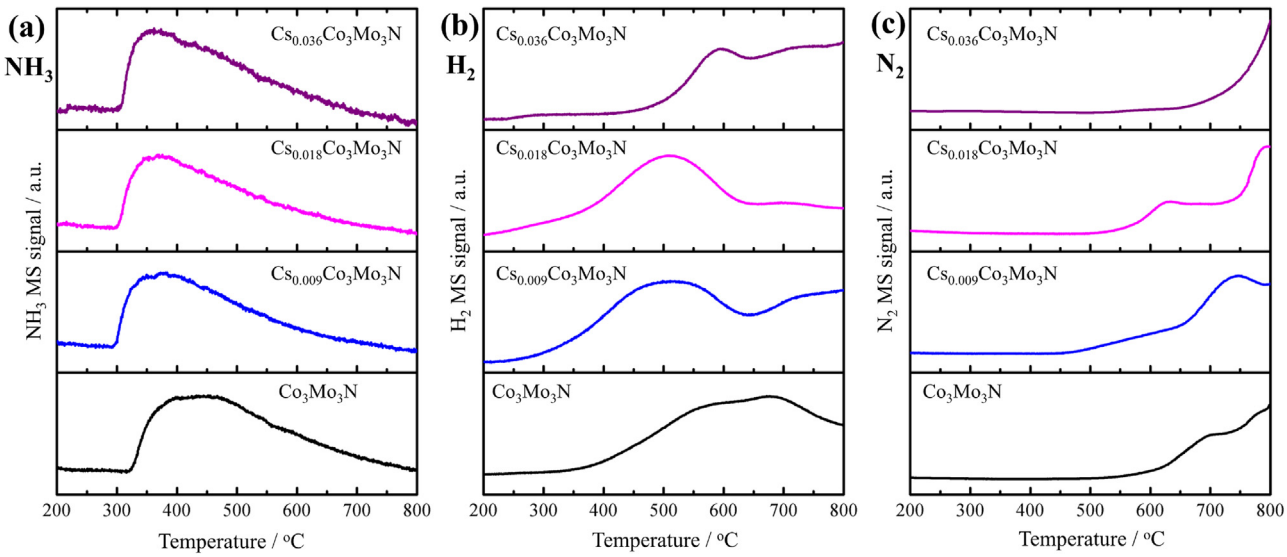

Fig. 9. (a) Ammonia (m/z = 17), (b) hydrogen (m/z = 2), and (c) nitrogen (m/z = 28) profiles in ammonia temperature-programmed surface reaction over the Co_3Mo_3N, $Cs_{0.009}Co_3Mo_3N$, $Cs_{0.018}Co_3Mo_3N$, and $Cs_{0.036}Co_3Mo_3N$ catalysts.

alyst. Note that the addition of Cs into Co_3Mo_3N did not change the reaction process over the nitride catalyst, although the Cs modification improved the activity of Co_3Mo_3N.

3.4. Desorption processes of gas species over the Cs-modified Co_3Mo_3N catalysts

In order to clarify the effects of added Cs species on the desorption processes of the reactant and product species over the catalyst during the ammonia decomposition, the NH_3-TPSR measurements were conducted for the Co_3Mo_3N, $Cs_{0.009}Co_3Mo_3N$, $Cs_{0.018}Co_3Mo_3N$, and $Cs_{0.036}Co_3Mo_3N$ catalysts. A blank experiment without ammonia adsorption step was initially carried out for the unmodified sample to ensure the desorption behavior of hydrogen adsorbed on the catalyst surface during the pretreatment process, as well as to confirm the nitrogen generated from the decomposition of sample. The profiles of hydrogen (m/z = 2) and nitrogen (m/z = 28) for the unmodified Co_3Mo_3N sample from blank experiment are depicted in Fig. S7a and b, respectively. The desorption of hydrogen started at *ca.* 500 °C and became pronounced above 650 °C, suggesting the strong hydrogen adsorption onto the catalyst surface. Furthermore, the generation of nitrogen above 650 °C was attributed to the decomposition of Co_3Mo_3N catalyst. The XRD measurement confirmed that the Co_3Mo_3N sample was partially changed to metal species at 1000 °C (not shown).

The ammonia (m/z = 17), hydrogen (m/z = 2), and nitrogen (m/z = 28) profiles obtained by NH_3-TPSR measurements for each catalyst are shown in Fig. 9. In the ammonia profiles (Fig. 9a), an onset temperature of ammonia desorption was observed at 325 °C for the unmodified Co_3Mo_3N and at 300 °C for all the Cs-modified Co_3Mo_3N catalysts. The ammonia desorption did not terminate even at 700 °C in both cases. These characteristics would be ascribable to the desorption behavior of ammonia on acidic sites of the catalysts. In addition, the mass signal of ammonia reached a maximum at 430 °C for the unmodified catalyst, whereas all the modified catalysts attained a peak signal at 370–390 °C. These findings suggested that ammonia more strongly adsorbed on the catalyst surface for the unmodified catalyst than for all the modified catalysts.

The desorption profiles of hydrogen for the unmodified and modified catalysts are shown in Fig. 9b. For the unmodified sample, a broad desorption peak of hydrogen was observed above 350 °C. The hydrogen desorption temperature depended on the amount of Cs additive. The hydrogen desorption was composed of two processes at 300–620 °C and above 650 °C for the modified catalysts with molar ratios of Cs/Co_3Mo_3N of 0.009 and 0.018. Judging from the hydrogen desorption in the blank measurement, the former was related to the hydrogen generation from ammonia decomposition over the catalyst, whereas the hydrogen strongly adsorbed onto the catalyst surface could be detected as the latter process. On the other hand, when the molar ratio of Cs to Co_3Mo_3N was further increased to 0.036, the signal of hydrogen reached a maximum at ca. 590 °C and maintained almost a constant value at higher temperatures. Similarly, the hydrogen desorption below 650 °C could be associated with ammonia decomposition. These results revealed that the generated hydrogen atoms weakly-adsorbed on the catalyst surface for the Co_3Mo_3N modified by Cs species with the low contents. It has been reported previously that the hydrogen strongly-adsorbed on the active site inhibits the ammonia decomposition reaction because it occupies the active site over the Ni and Ru-based catalysts [6,19–21]. Thus, the hydrogen desorption at low temperatures is desirable for the ammonia decomposition reaction. Therefore, it can be concluded that the modification of Co_3Mo_3N by a small amount of Cs species facilitated the hydrogen desorption process, resulting in the enhancement of its ammonia decomposition activity.

In the nitrogen profiles, as shown in Fig. 9c, the generation of nitrogen started at 500 °C for $Cs_{0.009}Co_3Mo_3N$ and $Cs_{0.018}Co_3Mo_3N$, at 560 °C for the unmodified Co_3Mo_3N, and at 650 °C for $Cs_{0.036}Co_3Mo_3N$. As mentioned above, the generation of nitrogen at the temperatures higher than 650 °C should be ascribable to the decomposition of Co_3Mo_3N catalyst. Thus, the nitrogen detected at lower temperatures would be derived from the ammonia decomposition. As in the case of hydrogen desorption, the nitrogen desorption at lower temperatures is desirable for ammonia decomposition. It has been reported that the Ru-based catalysts modified by cesium species are well known to be highly active for ammonia decomposition [5,10,16]. The cesium species act as an electron-donating promoter. The addition of this promoter can facilitate the nitrogen desorption process, leading to the enhancement of ammonia decomposition activity [10,16]. It should be possibly noted that the addition of a small amount of Cs promoted the nitrogen desorption step in ammonia decomposition reaction in this study.

As summarized in Table 2, the apparent activation energy of the modified samples was lower than the unmodified sample, except for $Cs_{0.036}Co_3Mo_3N$. This would correspond to the promotion of recombinative desorption of hydrogen and nitrogen atoms from catalyst surface by the addition of a small amount of Cs into Co_3Mo_3N catalysts. Furthermore, the high turnover frequency (TOF) over the modified catalyst was associated with the significant promotion of the ammonia decomposition reaction by the Cs species (Table 2).

4. Conclusion

A facile single-step synthesis of the Cs-modified Co_3Mo_3N catalysts was successfully demonstrated by the decomposition of the mixture containing HMTA and corresponding metal salts under the flow of nitrogen at 700 °C and their catalytic activity for ammonia decomposition was examined. The as-calcined samples were mainly composed of the Co_3Mo_3N phase with the existence of the Cs species. The catalytic activity of Co_3Mo_3N for ammonia decomposition was significantly improved by the addition of a small amount of Cs species. In addition, an excess amount of Cs species had a negative effect on catalytic performance for the reaction. This implied that the Cs species seemed to partially cover the active Co_3Mo_3N sites. The Cs-modified Co_3Mo_3N with mole ratios of Cs to Co_3Mo_3N of 0.009 and 0.018 exhibited the highest activity for ammonia decomposition. $^{15}NH_3$ isotopic studies provided the reaction mechanism over Co_3Mo_3N catalyst that the nitrogen species in the catalyst could be exchanged with the nitrogen atoms in the gaseous ammonia. In addition, a small amount of Cs species weakened the negative effect of the hydrogen poisoning on the active sites of Co_3Mo_3N according to the kinetics analyses. The NH_3–TPSR experiments suggested that the Cs modification facilitated the recombinative desorption of hydrogen and nitrogen atoms from the active components. This improvement could be associated with the electronic modification of Co_3Mo_3N by the electron donating Cs promoter.

Acknowledgments

This work was supported by Council for Science, Technology and Innovation (CSTI), Cross-ministerial Strategic Innovation Promotion Program (SIP), “Energy Carrier” (Funding agency: JST).

Appendix A. Supplementary data

Supplementary data associated with this article can be found, in the online version, at http://dx.doi.org/10.1016/j.apcatb.2017.06.034.

References

[1] C.H. Christensen, T. Johannessen, R.Z. Sørensen, J.K. Nørskov, Catal. Today 111 (2006) 140–144.
[2] R. Metkemeijer, P. Achard, J. Power Sources 49 (1994) 271–282.
[3] D.A. Hansgen, D.G. Vlachos, J.G. Chen, Nat. Chem. 2 (2010) 484–489.
[4] T. Matsui, S. Suzuki, Y. Katayama, K. Yamauchi, T. Okanishi, H. Muroyama, K. Eguchi, Langmuir 31 (2015) 11717–11723.
[5] K. Nagaoka, T. Eboshi, N. Abe, S.-i. Miyahara, K. Honda, K. Sato, Int. J. Hydrogen Energy 39 (2014) 20731–20735.
[6] K. Okura, T. Okanishi, H. Muroyama, T. Matsui, K. Eguchi, Appl. Catal. A 505 (2015) 77–85.
[7] S. Podila, S.F. Zaman, H. Driss, Y.A. Alhamed, A.A. Al-Zahrani, L.A. Petrov, Catal. Sci. Technol. 6 (2016) 1496–1506.
[8] S.-F. Yin, Q.-H. Zhang, B.-Q. Xu, W.-X. Zhu, C.-F. Ng, C.-T. Au, J. Catal. 224 (2004) 384–396.
[9] S. Podila, H. Driss, S.F. Zaman, Y.A. Alhamed, A.A. AlZahrani, M.A. Daous, L.A. Petrov, J. Mol. Catal. A: Chem. 414 (2016) 130–139.
[10] A.K. Hill, L. Torrente-Murciano, Int. J. Hydrogen Energy 39 (2014) 7646–7654.
[11] W. Zheng, J. Zhang, Q. Ge, H. Xu, W. Li, Appl. Catal. B 80 (2008) 98–105.
[12] H. Muroyama, C. Saburi, T. Matsui, K. Eguchi, Appl. Catal. A 443–444 (2012) 119–124.
[13] K. Okura, T. Okanishi, H. Muroyama, T. Matsui, K. Eguchi, ChemCatChem 8 (2016) 2988–2995.
[14] D. Varisli, E.E. Elverisli, Int. J. Hydrogen Energy 39 (2014) 10399–10408.
[15] B. Lorenzut, T. Montini, C.C. Pavel, M. Comotti, F. Vizza, C. Bianchini, P. Fornasiero, ChemCatChem 2 (2010) 1096–1106.
[16] A.K. Hill, L. Torrente-Murciano, Appl. Catal. B 172–173 (2015) 129–135.
[17] K. Okura, T. Okanishi, H. Muroyama, T. Matsui, K. Eguchi, RSC Adv. 6 (2016) 85142–85148.
[18] D.-C. Huang, C.-H. Jiang, F.-J. Liu, Y.-C. Cheng, Y.-C. Chen, K.-L. Hsueh, Int. J. Hydrogen Energy 38 (2013) 3233–3240.
[19] J. Zhang, H. Xu, W. Li, Appl. Catal. A 296 (2005) 257–267.
[20] A.S. Chellappa, C.M. Fischer, W.J. Thomson, Appl. Catal. A 227 (2002) 231–240.
[21] F. Hayashi, Y. Toda, Y. Kanie, M. Kitano, Y. Inoue, T. Yokoyama, M. Hara, H. Hosono, Chem. Sci. 4 (2013) 3124–3130.
[22] S. Wang, H. Ge, S. Sun, J. Zhang, F. Liu, X. Wen, X. Yu, L. Wang, Y. Zhang, H. Xu, J.C. Neuefeind, Z. Qin, C. Chen, C. Jin, Y. Li, D. He, Y. Zhao, J. Am. Chem. Soc. 137 (2015) 4815–4822.
[23] M. Nagai, Y. Goto, O. Uchino, S. Omi, Catal. Today 43 (1998) 249–259.
[24] D.-W. Kim, D.-K. Lee, S.-K. Ihm, Catal. Lett. 43 (1997) 91–95.
[25] E.J. Markel, J.W. Van Zee, J. Catal. 126 (1990) 643–657.
[26] J.A. Schaidle, L.T. Thompson, J. Catal. 329 (2015) 325–334.
[27] C.J.H. Jacobsen, Chem. Commun. (2000) 1057–1058.
[28] X. Duan, J. Ji, X. Yan, G. Qian, D. Chen, X. Zhou, ChemCatChem 8 (2016) 938–945.
[29] J. Ji, X. Duan, G. Qian, X. Zhou, G. Tong, W. Yuan, Int. J. Hydrogen Energy 39 (2014) 12490–12498.
[30] C. Liang, W. Li, Z. Wei, Q. Xin, C. Li, Ind. Eng. Chem. Res. 39 (2000) 3694–3697.
[31] C.S. Lu, X.N. Li, Y.F. Zhu, H.Z. Liu, C.H. Zhou, Chin. Chem. Lett. 15 (2004) 105–108.
[32] A. Srifa, K. Okura, T. Okanishi, H. Muroyama, T. Matsui, K. Eguchi, Catal. Sci. Technol. 6 (2016) 7495–7504.
[33] W. Zheng, T.P. Cotter, P. Kaghazchi, T. Jacob, B. Frank, K. Schlichte, W. Zhang, D.S. Su, F. Schüth, R. Schlögl, J. Am. Chem. Soc. 135 (2013) 3458–3464.
[34] S.T. Oyama, J. Catal. 133 (1992) 358–369.
[35] T.E. Bell, L. Torrente-Murciano, Top. Catal. 59 (2016) 1438–1457.
[36] X. Duan, G. Qian, X. Zhou, D. Chen, W. Yuan, Chem. Eng. J. 207–208 (2012) 103–108.
[37] B. Lorenzut, T. Montini, M. Bevilacqua, P. Fornasiero, Appl. Catal. B 125 (2012) 409–417.
[38] H. Wang, W. Li, M. Zhang, Chem. Mater. 17 (2005) 3262–3267.
[39] T. Chukeaw, A. Seubsai, P. Phon-in, K. Charoen, T. Witoon, W. Donphai, P. Parpainainar, M. Chareonpanich, D. Noon, B. Zohour, S. Senkan, RSC Adv. 6 (2016) 56116–56126.
[40] G. Zhang, H. Zhang, D. Yang, C. Li, Z. Peng, S. Zhang, Catal. Sci. Technol. 6 (2016) 6417–6430.
[41] M. Kruk, M. Jaroniec, Chem. Mater. 13 (2001) 3169–3183.
[42] N. Perret, A.-M. Alexander, S.M. Hunter, P. Chung, J.S.J. Hargreaves, R.F. Howe, M.A. Keane, Appl. Catal. A 488 (2014) 128–137.
[43] W. Zheng, J. Zhang, H. Xu, W. Li, Catal. Lett. 119 (2007) 311–318.